LAWRENCE
LIVERMORE
NATIONAL
LABORATORY

LLNL-CONF-406735

Smoothness monitors for compressible flow computation

B. Sjogreen, H. C. Yee

September 3, 2008

5th International Conference on Computational Fluid Dynamics
Seoul, South Korea
July 7, 2008 through July 11, 2008

Disclaimer

Smoothness monitors for compressible flow computation

Bjorn Sjogreen[1] and H.C.Yee[2]

[1] Lawrence Livermore National Laboratory sjogreen2@llnl.gov
[2] NASA Ames Research Center helen.m.yee@nasa.gov

Abstract: In [SY04, YS07] and references cited therein, the authors introduced the concept of employing multiresolution wavelet decomposition of computed flow data as smoothness monitors (flow sensors) to indicate the amount and location of built-in numerical dissipation that can be eliminated or further reduced in shock-capturing schemes. Studies indicated that this approach is able to limit the use of numerical dissipation with improved accuracy compared with standard shock-capturing methods. The studies in [SY04, YS07] were limited to low order multiresolution redundant wavelets with low level supports and low order vanishing moments. The objective of this paper is to expand the previous investigation to include higher order redundant wavelets with larger support and higher order vanishing moments for a wider spectrum of flow type and flow speed applications.

1 Redundant Wavelets

Assume that we are given a grid function u_j, $j = 1, \ldots, J$ on a grid $x_j = (j-1)\Delta x$. The goal is to detect regions where the grid function does not represent a smooth function on the scale Δx. In theory the degree of smoothness of a function can be deduced from its wavelet coefficients. Here, the basics of the redundant wavelet analysis is briefly summarized [D92]. The wavelet decomposition is more often defined without redundancy, i.e., as an expansion in basis functions, by localizing the wavelet coefficients at every second grid point. We then obtain J/2 wavelet coefficients and J/2 scaling function values. With this approach the regularity estimate at a grid point would depend on how the point is aligned with the coarsened grids. Furthermore, the regularity of the wavelet function itself would affect the maximum Lipschitz exponent (regularity estimate) that can be estimated [D92]. The wavelet decomposition is called redundant because we have computed 2J values at scale 1, namely the J wavelet coefficients $w_{1,j}$ and the J scaling functions $f_{1,j}$. This is more information than necessary to represent the original J grid function values.

Basic Wavelet Relations: The wavelet coefficient at x_j on scale m for a function $u(x)$ is defined by

$$w_{m,j}(u) = \int \psi_{m,j}(x)u(x)\,dx$$

where the wavelet function is

$$\psi_{m,j}(x) = \frac{1}{2^m}\psi((x - x_j)/2^m).$$

It is a scaled and translated version of a mother wavelet function $\psi(x)$. $\psi(x)$ is localized around $x = 0$. Associated with the wavelet function is a scaling function $\phi(x)$. Similar to the wavelet coefficients, the associated scaling function coefficients are,

$$f_{m,j}(u) = \int \phi_{m,j}(x)u(x)\,dx,$$

where $\phi_{m,j}(x) = 1/2^m\phi((x - x_j)/2^m)$. Furthermore $\phi(x)$ and $\psi(x)$ are such that the relations

$$\phi(x) = \sum_n a_n\phi(2x - n\Delta x) \qquad \psi(x) = \sum_n b_n\phi(2x - n\Delta x) \tag{1}$$

hold. The sums above are taken over a finite number of terms. Equations (1) give

$$w_{m+1,j} = \tfrac{1}{2}\textstyle\sum_n b_n f_{m,j+n2^m} := D(m)f_{m,j} \tag{2}$$
$$f_{m+1,j} = \tfrac{1}{2}\textstyle\sum_n a_n f_{m,j+n2^m} := A(m)f_{m,j}. \tag{3}$$

Thus, the wavelet and scaling coefficients on scale $m + 1$ are obtained by applying difference operators to the scaling coefficients on scale m. In (2) we denoted the wavelet operator on scale m by $D(m)$ to stress that this operator is usually a differentiation. The scaling function operator on level m, $A(m)$, is usually an averaging operator. The given grid x_j is at scale $m = 0$. The grid function u_j is given at this scale. No information is given about u_j on the smaller scales ($m < 0$). For the analysis of u_j, we usually approximate $f_{0,j} = u_j$. From $f_{0,j}$, equations (2) and (3) give $f_{m,j}$ and $w_{m,j}$ for all scales $m > 0$. We focus below on choices for $D(0)$ and $A(0)$. On the coarser scales (2) and (3) define $D(m)$ and $A(m)$ for $m > 0$.

Boundary Modification: For non-periodic boundaries, the difference operators need to be modified at the boundaries. We first do this at the grid scale $m = 0$ and then generalize the boundary modification to the coarser scales. Let the stencil of $D(0)$ be $p + q + 1$ points wide,

$$D(0)u_j = \sum_{n=-p}^{q} \frac{1}{2}b_n u_{j+n}, \qquad j = p + 1, \ldots, J - q.$$

To define $D(0)$ for all points x_j, $j = 1, \ldots, J$, we need boundary operators at the points $j = 1, \ldots, p$ with w the width of the operator,

$$D(0)u_j = \sum_{n=1}^{w} \beta_{j,n} u_n,$$

and similarly at the upper boundary. A natural choice is to let $\beta_{j,n}$ approximate the same quantity as is approximated by $D(0)u_j$ for $j > p$. At the coarser scales the stencil of $D(m)$ extends between $j - 2^m p$ and $j + 2^m q$. We define the generalization of the boundary operators to coarser scales by

$$D(m)u_j = \sum_{n=1}^{w} \beta_{l,n} u_{1+r+(n-1)2^m}, \qquad j = 1, \ldots, 2^m p,$$

where $l = [(j-1)/2^m] + 1$ and $r = j - 1 \bmod 2^m$ and where $[x]$ is the integer part of x obtained by truncating the decimals. The boundary modification of $D(m)$ at the upper boundary and the boundary modifications for $A(m)$ are defined similarly.

Vanishing Moments: A wavelet function has k vanishing moments if

$$\int x^n \psi(x)\, dx = 0, \quad n = 0, 1, 2, \ldots, k-1.$$

The wavelet theory says, see, e.g., [D92, MH92], that a redundant wavelet with k vanishing moments can be used to estimate the number of derivatives of a function, up to the kth derivative, because then the wavelet coefficients $w_{m,j}$ will depend on the scale as $2^{m\alpha}$, where $\alpha < k$ is the Lipschitz exponent of u_j near x_j. The test cases below illustrate the B-spline and the redundant form of Harten multiresolution wavelets.

B-spline Wavelets: The Nth degree B-spline wavelet with k vanishing moments have a scaling function whose Fourier transform is

$$\hat{\phi}(\omega) = \left(\frac{\sin \omega/2}{\omega/2} \right)^N \tag{4}$$

and wavelet function with Fourier transform is

$$\hat{\psi}(\omega) = (i\omega)^k \left(\frac{\sin \omega/4}{\omega/4} \right)^{N+k}. \tag{5}$$

We assume that N and k are even numbers. Fourier transformation of (1), use of (4) and (5), and comparison with (2) lead to the difference operators

$$D(0) = (\Delta_+ \Delta_-)^{k/2} \qquad A(0) = (A_+ A_-)^{N/2},$$

where the forward and backward undivided difference operators are

$$\Delta_- u_j = u_j - u_{j-1} \qquad \Delta_+ u_j = u_{j+1} - u_j,$$

and the forward and backward averaging operators are

$$A_- u_j = (u_j + u_{j-1})/2 \qquad A_+ u_j = (u_{j+1} + u_j)/2.$$

The first operators are

$$\begin{aligned} A(0)u_j &= u_j && (N=0)\\ A(0)u_j &= (u_{j+1} + 2u_j + u_{j-1})/4 && (N=2)\\ A(0)u_j &= (u_{j+2} + 4u_{j+1} + 6u_j + 4u_{j-1} + u_{j-2})/16 && (N=4) \end{aligned}$$

and

$$\begin{aligned} D(0)u_j &= u_{j+1} - 2u_j + u_{j-1} && (k=2)\\ D(0)u_j &= u_{j+2} - 4u_{j+1} + 6u_j - 4u_{j-1} + u_{j-2} && (k=4). \end{aligned}$$

The wavelet operators are approximations of the kth derivative, e.g.,

$$u_{j+2} - 4u_{j+1} + 6u_j - 4u_{j-1} + u_{j-2} \approx \Delta x^4 u_{xxxx}(x_j).$$

The averaging operators $A(0)u_j$ are all second order accurate approximations of the point value u_j.

The operators for odd k or N are analogous. The wavelet operators are approximations of odd order derivatives centered at half points. For example, the operators with $k = 3$ are

$$\begin{aligned} A(0)u_{j+1/2} &= (u_{j+2} + 3u_{j+1} + 3u_j + u_{j-1})/8\\ D(0)u_{j+1/2} &= (u_{j+2} - 3u_{j+1} + 3u_j - u_{j-1}). \end{aligned}$$

Redundant Form of Harten Multiresolution Wavelets [SY04]: The idea is to use a kth order accurate average operator

$$A(0)u_j = u(x_j) + \mathcal{O}(\Delta x^k)$$

which does not make use of the value u_j. The wavelet operator is defined as

$$D(0)u_j = u_j - A(0)u_j$$

so that the wavelet coefficient at x_j is the difference between an interpolated value and the actual value. If this difference is small, we expect the function to be well-behaved. The first operators are

$$\begin{aligned} A(0)u_j &= (u_{j+1} + u_{j-1})/2 && (k=2)\\ A(0)u_j &= (-u_{j+2} + 4u_{j+1} + 4u_{j-1} - u_{j-2})/6 && (k=4) \end{aligned}$$

with corresponding wavelet operators,

$$D(0)u_j = \qquad -(u_{j+1} - 2u_j + u_{j-1})/2 \qquad (k = 2)$$
$$D(0)u_j = (u_{j+2} - 4u_{j+1} + 6u_j - 4u_{j-1} + u_{j-2})/6 \qquad (k = 4).$$

In general, the wavelet operator is the same as for the B-spline case, but normalized differently. The multiresolution wavelet allows the grid function to be decomposed,

$$u_j = A(0)u_j + D(0)u_j = A(1)A(0)u_j + D(1)A(0)u_j + D(0)u_j = \ldots$$

etc. into any number of scales.

Regularity Estimate: The grid size at scale m is $2^m \Delta x$. This implies that $(\Delta_- \Delta_+)^{k/2} u_j$ will depend on the scale as $(2^m \Delta x)^k = 2^{mk} \Delta x^k$ if u_j is sampled from a k times differentiable function. According to the theory, [D92, MH92], the local regularity should be measured over the domain of dependence of the point x_j. We define

$$d_{m,j} = \max\{|w_{m,n}| \ \ |n : j \ \text{ in stencil for } \ w_{m,n}\}.$$

If $d_{m,j}$ depend on the scale as $2^{\alpha m}$, then α is the local Lipschitz exponent at x_j of the analyzed function. We use a least squares fit to the model $\log_2 d_{m,j} = \alpha m + c$ to estimate the slope α. With two, three, and four scales this gives the estimates

$$\alpha \approx \log_2(d_{1,j}/d_{0,j}),$$
$$\alpha \approx \frac{1}{2} \log_2(d_{2,j}/d_{0,j}),$$

and

$$\alpha \approx (3 \log_2(d_{3,j}/d_{0,j}) + \log_2(d_{2,j}/d_{1,j}))/10$$

respectively. It is also necessary to avoid division by zero and/or taking the logarithm of zeros. Therefore, if $|w_{m,j}| < 2^{mk}\epsilon$, we set $w_{m,j}$ to $2^{mk}\epsilon$ for some given tolerance ϵ.

2 Test Cases

Due to space limitation, as an illustration, we select for any non-negative even numbers N and k, the B-spline wavelet operator pair

$$D(0) = (\Delta x^2 D_+ D_-)^{k/2} \quad A(0) = (A_+ A_-)^{N/2}$$

and the multiresolution wavelet operator pair

$$D(0) = \frac{1}{d_0}(\Delta x^2 D_+ D_-)^{k/2} \quad A(0) = I - D(0),$$

where d_0 is the coefficient in front of u_j in $(\Delta x^2 D_+ D_-)^{k/2}$. We will test these operators for different values of k and N, and for different number of scales.

Examples using the redundant form of Harten multiresolution wavelets will be reported in a forthcoming article.

Performance of Smoothness Monitors using B-Splines on a Given Data: The given data indicates in the top left of Fig. 1 is the density of a computed solution of a standard 1-D inviscid shock-turbulence interaction test case in gas dynamics. A Mach 3 shock moves to the right into a sinusodial entropy wave. The interaction amplifies the entropy waves and creates acoustic waves behind the shock. Oscillations of higher frequency develop. A few weaker shocks are located behind the acoustic wave region. The solution (given data) in Fig. 1a was computed by the 5th-order WENO scheme on a very fine grid. A good detector should be able to detect the leading shock wave, but classify the physical oscillations ($0.5 < x < 2.2$ and $x > 2.2$) as smooth regions. Samples of estimated regularity exponents are shown in Figs. 1b–1d with the original function shown in black. We investigate the influence of the parameters N, k, and the number of scales (or levels) used for the B-spline wavelets. In all experiments shown, $\epsilon = 10^{-3}$. Figure 1b shows that the estimated α becomes smaller when the B-spline order N is increased. Note that the oscillatory part is classified as regular. In figure 1c, we vary the number of levels (or scales) from two to four. The estimated α becomes lower when the number of levels increases at the oscillations, but at the jumps the estimated α is higher for a larger number of levels. Finally, Fig. 1d shows the α estimate for $k = 2$ and $k = 4$ with N and the number of levels unchanged. Here α is larger for $k = 4$, except at the jump where α is almost unchanged. The influence of the number of vanishing moments is clearly visible for the oscillations. The trends in Figs. 1b–1d were the same for all choices of the fixed parameters. At shock locations, the higher the N, k and L values, the lower the value of α's (near zero or negative spikes). At the physical oscillation region, for all of the studied N, k and L values, the values of α remain positive for the entire region (above 2 in this case). As a second test case to examined how the α behaves at regions of spurious high frequency oscillations (completely due to the numerics), we examined the regularity of the data obtained from the pure convection of a 2-D vortex (inviscid) by the 8th-order central spatial scheme without numerical dissipation added. In this case the exact solution is smooth and a good scheme is expected to convect the vortex without distortion for certain reasonable time lengths. Due to the lack of numerical dissipation and the nonlinearity of the Euler equations, in this case, spurious high frequency oscillation occurs at very early stages of time evolution. The oscillation becomes more pronounced as time progresses and the solution eventually diverges. The data we obtained is at the early stage of the spurious high frequency oscillation. We examined the same N, k and L values. It turns out that at the spurious high frequency oscillation regions, unlike physical oscillations, the αs in this entire region are negative. Thus, the use of α as a flow sensor is a clear cut indication on the locations of shocks, physical oscillations and spurious high frequency oscillations.

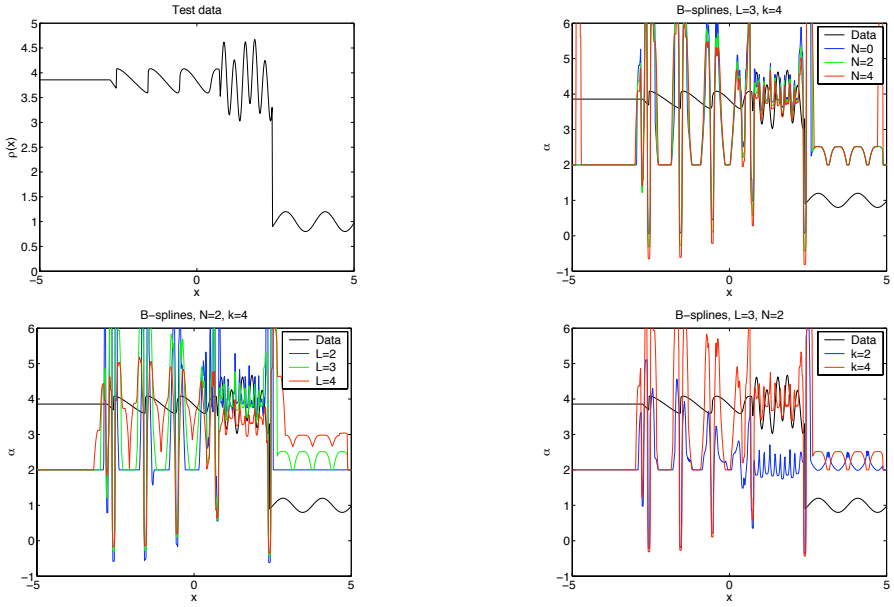

Fig. 1. a) (top left) Test function with jumps and smooth oscillations. b) (top right) Estimated α when the B-spline order N varies . c) (bottom left) Estimated α when the number of wavelet levels varies. d) (bottom right) Estimated α when the number of vanishing moments, k, varies.

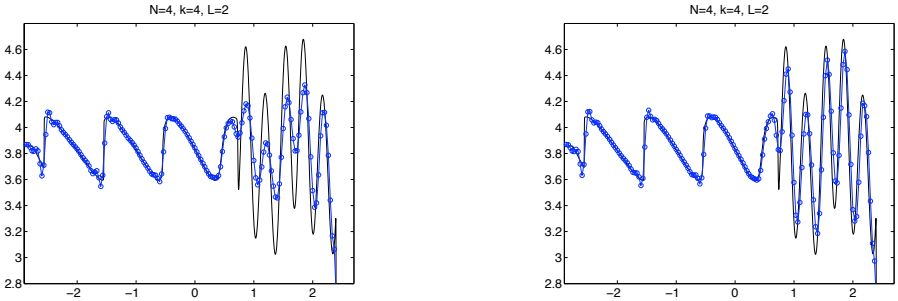

Fig. 2. a) (left) Density by the filter scheme using B-spline wavelet with $N = 2, k = 2, L = 2$ as a flow sensor. b) (right) Density by the filter scheme using B-spline wavelet with $N = 4, k = 4, L = 2$ as a flow sensor.

High Order Filter schemes with Flow Sensors as Part of the Definition of the Filter Numerical Dissipation: The term "smoothness monitor" or "flow sensor" used here is different from a limiter in the sense that, in addition to the built-in limiter existing in shock-capturing schemes, we use a flow sensor as an adaptive procedure to analyze the computed data to indicate the amount and location of built-in numerical dissipation that can be eliminated or further reduced. For a chosen numerical dissipation term, after incorporating the flow sensor as part of the definition of the numerical dissipation, a less dissipative numerical dissipation model emerges. The improved numerical dissipation model can be used as the replacement of the existing numerical dissipation term. Alternatively, the improved dissipation model can be used to construct a new scheme. An efficient approach is to apply the improved numerical dissipation model as a filter step in conjunction with high order non-dissipative central (compact or non-compact) spatial base schemes. Figure 2 shows the solution of the same 1-D shock-turbulence problem computed by the filter scheme with the 8th-oder central spatial base scheme and the dissipative portion of a 2nd-order TVD scheme as part of the filter with $N = 2, k = 2, L = 2$ and $N = 4, k = 4, L = 2$ as B-spline wavelet flow sensors. The limiter is the van Albada limiter for the nonlinear field and super B limiter for the linear field. The slight oscillation around the weak shock regions is typical of the super B limiter effect. The results indicate that higher order N and k values provide higher accuracy solution in the physical oscillation region with similar accuracy around the shock regions. With this adaptive numerical dissipation control of our filter scheme, the accuracy is comparable to a 7th-order WENO scheme using the same grid, and yet requires more than double the CPU time.

Concluding Remarks: The above test cases indicate that the use of multiresolution redundant wavelet decomposition of computed data is a good smoothness monitor with distinct characteristics of Lipschitz exponent for shocks, physical oscillation and spurious high frequency oscillation (due to the numerics). The smoothness monitors are useful as data analysis and as part of an improved numerical dissipation model or filter scheme. More detail studies, including 3-D Navier-Stokes computations will be reported in a forthcoming article.

References

[D92] Daubechies, I.: Ten Lectures on Wavelets. SIAM (1992).

[MH92] Mallat, S. and Hwang, W.L.: Singularity Detection and Processing with Wavelets. IEEE Trans. Inform. Theory, **38**, 617–643 (1992)

[SY04] B. Sjögreen and H. C. Yee, Multiresolution Wavelet Based Adaptive Numerical Dissipation Control for Shock-Turbulence Computation, J. Scient. Computing, **20**, 211-255 (2004).

[YS07] H.C. Yee and B. Sjögreen, Development of Low Dissipative High Order Filter Schemes for Multiscale Navier-Stokes/MHD Systems, J. Comput. Phys., 225 910-934 (2007).

This work performed under the auspices of the U.S. Department of Energy by Lawrence Livermore National Laboratory under Contract DE-AC52-07NA27344.